ISBN: 978-3-95450-219-6 ISSN: 2226-0366 doi: 10.18429/JACoW-LINAC2024-TUPB076

BEAM TRANSIENT STUDIES FOR THE JAEA-ADS LEBT

B. Yee-Rendon*, Y. Kondo, J. Tamura, F. Maekawa, S. Meigo
Japan Atomic Energy Agency (JAEA), Tokai, Japan

Abstract

The Japan Atomic Energy Agency (JAEA) is designing a 30-MW CW proton linear accelerator (linac) for nuclear waste transmutation. Space-charge is the primary challenge in achieving low losses and high beam quality for high-power accelerators, especially at low energy levels where space-charge forces are greater. To counteract the space-charge effects, the low-energy beam transport (LEBT) uses a magnetostatic design to enable the neutralization of the beam charge, the so-called space charge compensation. The neutralization is an accumulation process that reaches a charge balance between the main beam and the opposite ionized particles. However, this equilibrium is destroyed by the chopper system used during beam ramping. During those transient regimes, the beam optics conditions are not optimal for the beam, producing considerable degradation that can end in serious damage to the accelerator. Thus, analysis of beam behavior at these periods is essential to develop a robust design and an efficient operation of the JAEA-ADS linac. This study presents the beam dynamics of neutralization build-up and chopper operation for the JAEA-ADS LEBT.

INTRODUCTION

The Japan Atomic Energy Agency (JAEA) is designing an accelerator-driven subcritical system (ADS) for nuclear waste transmutation [1]. To this end, JAEA will use a 30-MW continuous-wave superconducting proton linear accelerator [2]. As with any high-intensity accelerator, space charge is the main challenge to avoid beam losses. Therefore, the low-energy beam transport (LEBT) uses a space charge compensation (SCC) design [3] to transport the beam from the ion source to the RFQ to avoid large emittance growth caused by space-charge effects. SCC occurs when the main beam ionizes the residual gas, producing secondary particles. These secondary particles with an opposite charge regarding the main beam are trapped in the beam potential and accumulate until reaching a steady equilibrium state. This leads to a screening of the space charge forces.

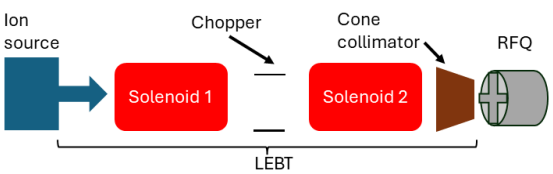

Figure 1: Schematic view of the JAEA-ADS LEBT design.

Figure 1 and Table 1 show the LEBT design and its main parameters, respectively. In this design, the chopper is placed between the solenoids, bringing solenoid 2 closer to RFQ to achieve a more convergent beam.

Table 1: Main Parameters for the JAEA-ADS LEBT

Parameter	
Particle	Proton
Beam current (mA)	25
Beam energy (keV)	35
Solenoid length (mm)	300
Solenoid 1 position (mm)	500
Solenoid 2 position (mm)	1680
Chopper length (mm)	125
Chopper position (mm)	1347.5
Length (mm)	1960

Previous LEBT model [4] considered a piecewise constant space-charge compensation. However, experiments and studies show a more complex profile [3,5]. Thus, this work improves the accuracy of SCC by developing a time-dependent LEBT model utilizing Warp [6] to include the ionization process. Furthermore, beam transient analysis will be utilized to determine the beam structure for nominal operation by taking into account the conditions needed to reach a steady state and the beam power ramp strategies by investigating the chopper effects.

BEAM TRANSIENT STUDIES

Transient beam studies were conducted using Warp, a 3D particle-in-cell program developed at Lawrence Berkeley National Laboratory to model high-intensity beams [7–9]. Warp is a self-consistent code, which means it can accurately simulate space charge effects in the beams.

In SCC studies, the SCC level (η) is a standard figure of merit used to evaluate the reduction in the effect of the current space charge. η is quantified as [10]:

$$\eta = 1 - \frac{\#\text{ negative particles}}{\#\text{ positive particles}}, \tag{1}$$

where # of charged particles that are contained to a certain root-means square (rms) beam size.

Another important variable is the SCC transient time (τ_{scc}), which provides information about the time required for a particle of the beam to produce a neutralizing particle in the residual gas. τ_{scc} is defined as [3,5]:

$$\tau_{\text{scc}} = \frac{kT}{\sigma_{\text{gas}} P v_b}, \tag{2}$$

where σ_{gas} is the cross-section of the beam particle to the residual gas, k is the Boltzmann constant, T is the tempera-

* byee@post.j-parc.jp

ISBN: 978-3-95450-219-6 ISSN: 2226-0366 doi: 10.18429/JACoW-LINAC2024-TUPB076

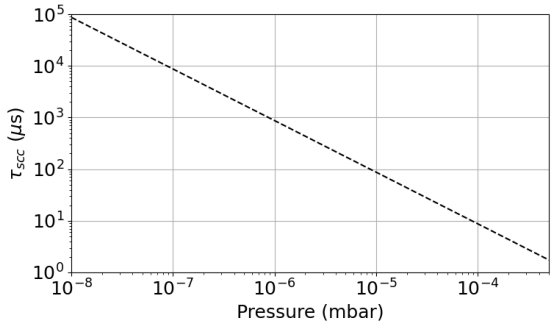

Figure 2: τ_{scc} for a 35 keV proton beam as a function of the pressure using H_2 as residual gas at room temperature.

ture of the residual gas, P is the pressure, and v_b is the beam speed. For our LEBT, a proton beam of 35 keV with a velocity of $v_b = 2.5 \times 10^6$ m/s. Considering H_2 as the residual gas, σ_{gas} =1.8 $\times 10^{-2}$ m^{-2}. The τ_{scc} as a function of the pressure is shown in Fig. 2. LEBT studies agree that takes about 2 to 3 $\times \tau_{scc}$ to reach the SCC steady state.

LEBT TUNING

During LEBT tuning, the solenoids were adjusted to achieve beam size and orientation for RFQ beam transmission greater than or equal to 95%. Table 2 provides information on the Warp simulations. For this analysis, I considered only the secondary electrons produced by the ionization of H_2 gas by the beam. Table 2 provides a summary of Warp simulations. Additional beam parameters and details of the LEBT elements are given in Table 1. Since H_2 was used as the residual gas, a pressure value of 1 $\times 10^{-4}$mbar was chosen to have a practicable SCC (τ_{scc}) of 8.88 μs (see Fig. 2) to reduce the computational cost time. Similarly, the beam particles injected per pass were approximately 12000, as a trade-off to minimize numerical heating effects and a manageable computational time.

Figure 3 shows η along the LEBT at different times, while Fig. 4 shows transverse-profile evolution for two of those times. At 10 μs (1.1 $\times \tau_{scc}$) the SCC level is close to 80% between the solenoids, then slowly increases to reach an SCC of 92%. There are small differences in the SCC in the solenoid areas between 20 μs (2.2 $\times \tau_{scc}$) and 30 μs (3.4 $\times \tau_{scc}$), however, scanning the solenoid, Fig. 5, indicates that at 30 μs the values have reached some convergence.

Table 2: Warp Simulations Details

Parameter	
Beam particle	proton
Residual gas	H_2
Pressure (mbar)	1 $\times 10^{-4}$
τ_{scc} (μs)	8.88
Simulation time (μs)	30 (3.4 $\times \tau_{scc}$)
Injected macro beam particles per step	11811
Time step (ns)	0.1
Smallest mesh resolution (mm)	0.5 × 0.5 × 0.5

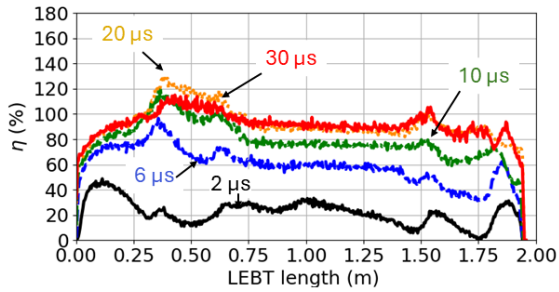

Figure 3: Buildup of the SCC along the LEBT.

The effectiveness of the SCC to control the beam size is shown in Fig. 4. At the top part, the horizontal distribution at 2 μs when the SCC is 20% on average, and on the bottom, when the steady state is reached. The LEBT tuning consisted of the scan of the two solenoids, where the emittance, Twiss parameters, and beam current were computed. Figure 5 displays the results of the Solenoid 1 scan (from 185 mT to 195 mT) when the field of Solenoid 2 was 243 mT. Small fields from Solenoid 1 result in larger beams entering Solenoid 2, which, at a fixed field, cannot make the beam converge any further. Increasing the field from Solenoid 1 makes the beam smaller, resulting in a more convergent beam. However, varying the beam size and solenoid fields affects the trapped electrons and consequently the SCC. This can be observed with some delay in the convergence of the emittance (Fig. 5(a)) and in achieving full current transmission (Fig. 5(b)).

The beam distribution and parameters obtained from Warp were used as input data for the JAEA-ADS RFQ model [11]. In Fig. 6, it is shown that for field values of 191 mT and 243 mT for the solenoid and 2, respectively, the RFQ transmission is greater than 95%. As a result, these solenoid values were chosen for the LEBT model.

CHOPPER STUDY

The chopper is designed to control the beam pulse length to increase the beam power. However, the chopper's opera-

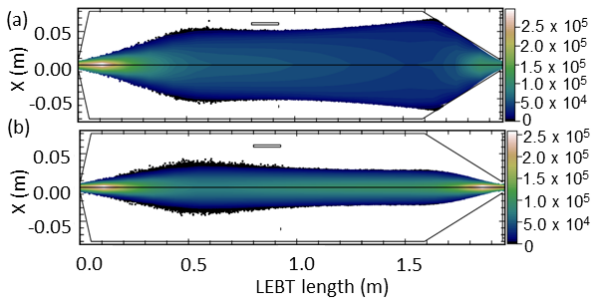

Figure 4: Beam horizontal distribution along the LEBT at two times: (a) after 2 μs and (b) 30 μs from the beginning of the simulation.

ISBN: 978-3-95450-219-6 ISSN: 2226-0366 doi: 10.18429/JACoW-LINAC2024-TUPB076

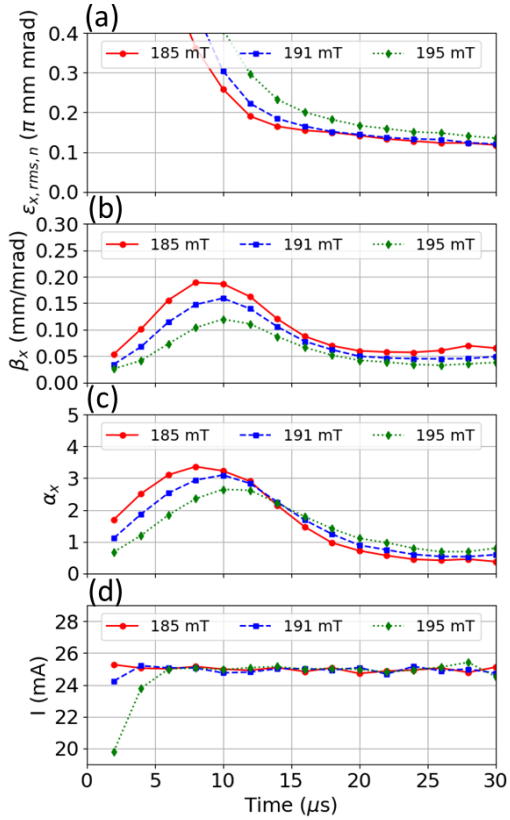

Figure 5: Transients of the emittance (a), β Twiss (b), α Twiss (c), and beam current (d) for different fields of Solenoid 1. Solenoid 2 was fixed to a value of 243 mT.

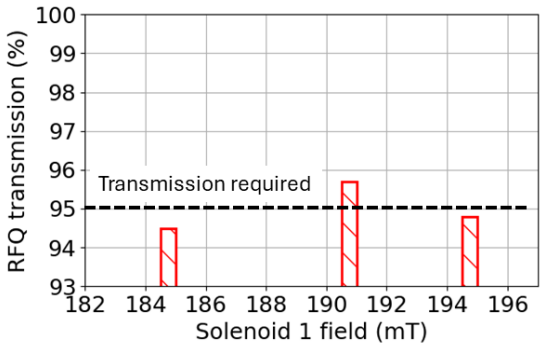

Figure 6: RFQ transmission for different Solenoid 1 fields. The black-dotted line shows the transmission required

tion not only removes the proton beam but also the trapped electron, which destroys the SCC. Consequently, the beam will need a certain time to restore the SCC conditions. This effect was simulated using as the start point the steady-state obtained during the LEBT tuning. Table 3 presents additional details for the chopper studies. Figure 7 shows the transient effect of the beam on the emittance and beam current. The yellow rectangle indicates when the chopper is on. After the chopper is turned off, it takes about 6 µs to fully recover transmission, but it took 20 µs to achieve an emittance level similar to the steady state. A detailed chopper study was reported in a previous conference [12].

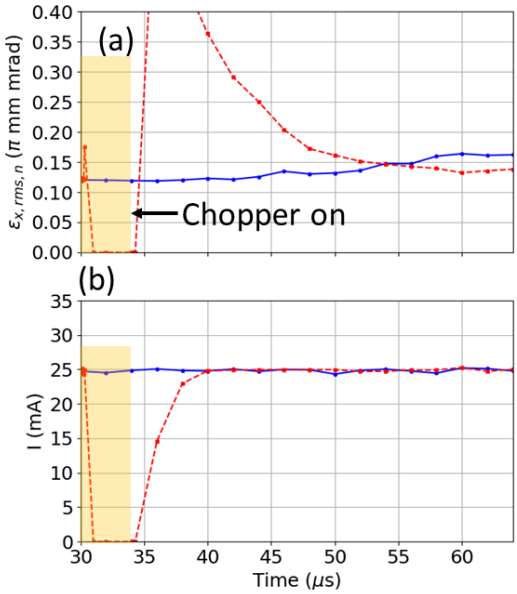

Figure 7: Transients of the emittance (a) and current for the case with and without chopper. The chopper was on by 4 µs and then was tracking from another 30 µs.

Table 3: Chopper Simulations Details. In addition to the parameters presented in Table 2. The simulation time starts from the steady state in the LEBT tuning, i.e., after 30 µs.

Parameter		
Chopper voltage (kV)		4
Simulation time (µs):		34
	Chopper on	4
	Chopper off	30

CONCLUSIONS

The present JAEA-ADS LEBT model allows a more accurate simulation of the space-charge compensation for the tuning of solenoid positions and fields to achieve compensation level about 92% and over 95% RFQ transmission. Beam simulations demonstrated that downstream transmission to the target met the design's performance requirements. In addition, chopper studies conclude that a 4 kV voltage can fully dump the beam. The transient time to recover steady conditions is higher than $2 \times \tau_{scc}$. As a next step, we will explore additional conditions such as varying residual gases and pressures to enhance the model.

ACKNOWLEDGMENTS

The authors thank Tomonobu Itagaki, Kai Masuda, and Nicolas Chauvin, for their valuable help with the Warp code. Kazou Hiyama, for his help installing the Warp code on the supercomputer. This research was conducted with the supercomputer HPE SGI8600 in the Japan Atomic Energy Agency. This work is supported by JSPS KAKENHI Grant Number 24H00235.

ISBN: 978-3-95450-219-6 ISSN: 2226-0366 doi: 10.18429/JACoW-LINAC2024-TUPB076

REFERENCES

[1] T. Sugawara *et al.*, "Research and development activities for accelerator-driven system in JAEA", *Prog. Nucl. Energy*, vol. 106, p. 27, Feb. 2018. doi:10.1016/j.pnucene.2018.02.007

[2] B. Yee-Rendon *et al.*, "Design and beam dynamic studies of a 30-MW superconducting linac for an accelerator-driven subcritical system", *Phys. Rev. Accel. Beams.*, vol. 24, p. 120101, Dec. 2021. doi:10.1103/PhysRevAccelBeams.24.120101

[3] O. Delferrière, R. D. Duperrier, D. Uriot, N. Chauvin, R. Gobin, and P. A. P. Nghiem, "Source and injector design for intense light ion beams including space charge neutralisation", in *Proc. LINAC'10*, Tsukuba, Japan, Sep. 2010, paper TH302, pp. 740–744.

[4] B. Yee-Rendon *et al.*, "Design of the low energy beam transport line for the JAEA-ADS linac", in *Proc. of the PASJ2023*, Funabashi, Japan, Aug. 2023, WEP23, pp. 545-549.

[5] C. A. Valerio *et al.*, "Negative ion beam space charge compensation by residual gas", *Phys. Rev. Accel. Beams.*, vol. 18, p. 080101, Dec. 2015. doi:10.1103/PhysRevAccelBeams.18.080101

[6] A. Friedman *et al.*, "Computational methods in the WARP code framework for kinetic simulations of particle beams and plasmas", *IEEE Trans. Plasma Sci.*, vol. 42, p. 1321, June 2013. doi:10.1109/PLASMA.2013.6633427

[7] L. Bellan *et al.*, "Space charge and electron confinement in high current low energy transport lines: Experience and Simulations From IFMIF/EVEDA and ESS Commissioning", in *Proc. LINAC'22*, Liverpool, UK, Aug.-Sep. 2022, pp. 618–621. doi:10.18429/JACoW-LINAC2022-TUPORI29

[8] N. Chauvin, O. Delferriere, R. Gobin, P. A. P. Nghiem, D. Uriot, and R. D. Duperrier, "Simulations and measurements in high intensity LEBT with space charge compensation", in *Proc. HB'12*, Beijing, China, Sep. 2012, paper THO3A03, pp. 507–510.

[9] K. Masuda *et al.*, "Commissioning of IFMIF prototype accelerator towards CW operation", in *Proc. LINAC'22*, Liverpool, UK, Aug.-Sep. 2022, pp. 319–323. doi:10.18429/JACoW-LINAC2022-TU2AA04

[10] N. Chauvin, T. Itagaki, and K. Masuda, private communication, Oct. 2023.

[11] Y. Kondo *et al.*, "Reference design of the RFQ for JAEA-ADS linac", in *Proc. J-PARC2019*, Tsukuba, Japan, vol. 33, p. 011015, March 2021. doi:10.7566/JPSCP.33.011015

[12] B. Yee-Rendon *et al.*, "Design and beam dynamics studies of a chopper for the JAEA-ADS LEBT", in *Proc. of the PASJ2024* (accepted for publication).